JOURNAL OF GEOPHYSICAL RESEARCH, VOL. 112, D10S34, doi:10.1029/2006JD007583, 2007

Effects of mixing on evolution of hydrocarbon ratios in the troposphere

D. D. Parrish,[1] A. Stohl,[2] C. Forster,[2] E. L. Atlas,[3] D. R. Blake,[4] P. D. Goldan,[1,5] W. C. Kuster,[1,5] and J. A. de Gouw[1,5]

Received 31 May 2006; revised 30 August 2006; accepted 1 November 2006; published 21 March 2007.

[1] Nonmethane hydrocarbon (NMHC) concentration ratios provide useful indicators of tropospheric oxidation and transport processes. However, the influences of both photochemical and mixing processes are inextricably linked in the evolution of these ratios. We present a model for investigating these influences by combining the transport treatment of the Lagrangian particle dispersion model FLEXPART with an ultrasimple (i.e., constant OH concentration) chemical treatment. Required model input includes NMHC emission ratios, but not ad hoc assumed background NMHC concentrations. The model results give NMHC relationships that can be directly compared, in a statistical manner, with measurements. The measured concentration ratios of the longest-lived alkanes show strong deviations from purely kinetic behavior, which the model nicely reproduces. In contrast, some measured aromatic ratio relationships show even stronger deviations that are not well reproduced by the model for reasons that are not understood. The model-measurement comparisons indicate that the interaction of mixing and photochemical processing prevent a simple interpretation of ''photochemical age,'' but that the average age of any particular NMHC can be well defined and can be approximated by a properly chosen and interpreted NMHC ratio. In summary, the relationships of NMHC concentration ratios not only yield useful measures of photochemical processing in the troposphere, but also provide useful test of the treatment of mixing and chemical processing in chemical transport models.

Citation: Parrish, D. D., A. Stohl, C. Forster, E. L. Atlas, D. R. Blake, P. D. Goldan, W. C. Kuster, and J. A. de Gouw (2007), Effects of mixing on evolution of hydrocarbon ratios in the troposphere, *J. Geophys. Res.*, *112*, D10S34, doi:10.1029/2006JD007583.

1. Introduction

[2] Nonmethane hydrocarbons (NMHC) are ubiquitous trace species of the troposphere that provide useful indicators of atmospheric oxidation and transport processes. Both anthropogenic and natural sources emit NMHC. These sources are widely dispersed, primarily at the surface over continents. In situ oxidation processes, predominately those initiated by the hydroxyl radical (OH), convert the emitted NMHC to a variety of partially oxidized organic species, and ultimately to carbon dioxide and water. Figure 1 shows the rates of the initial oxidation by OH for some of the more common and less reactive NMHC. Since these reaction rates span several orders of magnitude, as air is transported away from a source that emitted NMHC into a particular air parcel, the NMHC are removed at different rates, and the concentration pattern of the NMHC changes. This concentration pattern change can, therefore, provide an indicator for the degree of photochemical processing or aging that has occurred in a sampled air parcel.

[3] No air parcel is ever transported and photochemically aged in isolation; atmospheric transport is always accompanied by dispersion and mixing, which also affect the NMHC concentration pattern. Many studies have utilized measured NMHC concentration patterns as indicators of photochemical processing. These studies have found that concentration ratios of NMHC with different rates of removal are particularly useful, because the ratios are less sensitive to dilution and mixing of air masses than are the absolute concentrations themselves. These studies have either neglected [*Calvert*, 1976; *Roberts et al.*, 1984, 1985; *Rudolph and Johnen*, 1990]; or through a variety of strategies approximately accounted [*Parrish et al.*, 1992; *McKeen and Liu*, 1993; *McKenna et al.*, 1995; *McKeen et al.*, 1996; *Ehhalt et al.*, 1998] for the confounding effects that mixing and dispersion have even on the concentration ratios.

[4] The NMHC measurements and model calculations from three recent field studies provide an opportunity to

[1]Earth System Research Laboratory, NOAA, Boulder, Colorado, USA.
[2]Department of Regional and Global Pollution Issues, Norwegian Institute for Air Research, Kjeller, Norway.
[3]Division of Marine and Atmospheric Chemistry, Rosenstiel School of Marine and Atmospheric Science, University of Miami, Miami, Florida, USA.
[4]Department of Chemistry, University of California, Irvine, California, USA.
[5]Also at Cooperative Institute for Research in Environmental Sciences, University of Colorado, Boulder, Colorado, USA.

0148-0227/07/2006JD007583$09.00

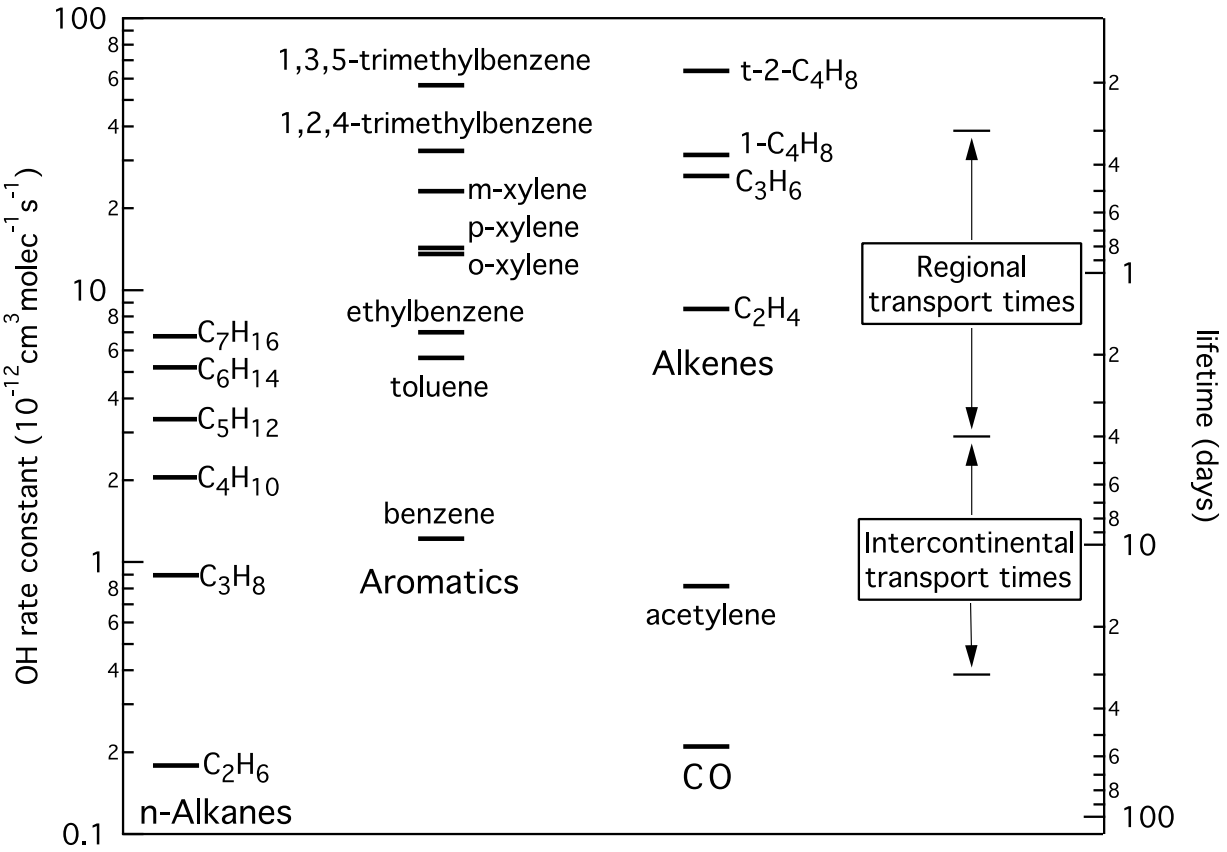

Figure 1. Rate constants and corresponding atmospheric lifetimes for some NMHC. Carbon monoxide is included for comparison. The approximate timescales for regional and intercontinental transport are indicated. NMHC rate constant data are from *Atkinson and Arey* [2003]. The lifetimes correspond to [OH] = 1×10^6 molecules cm^{-3}. (Figure closely follows that of *Parrish et al.* [1998].)

more quantitatively investigate the effects of mixing on evolution of hydrocarbon ratios in the troposphere. The International Consortium for Atmospheric Research on Transport and Transformation (ICARTT) study [*Fehsenfeld et al.*, 2006] was conducted in the summer of 2004 over eastern North America and the western North Atlantic and the Intercontinental Transport and Chemical Transformation (ITCT 2K2) study [*Parrish et al.*, 2004a] was conducted in 2002 over western North America and the eastern North Pacific in the spring of 2002. Both studies measured NMHC concentrations from several different platforms and ground sites. For these two studies the FLEXPART [*Stohl et al.*, 2005] Lagrangian particle dispersion model treated the anthropogenic CO emissions injected into the measured air masses and characterized the transport and dispersion of those air masses. The NEAQS 2002 study was conducted in the summer of 2002 in the Gulf of Maine off the northeast North American coast, and included shipboard NMHC measurements; FLEXPART calculations are not available for this study.

[5] This paper uses these NMHC measurements and FLEXPART calculations for two purposes. First the FLEXPART treatment of CO emissions is approximately adapted to NMHC emissions to examine the effect of dispersion and mixing on the NMHC ratios. The goal here is to determine how well model calculations can reproduce the relationships found between measured NMHC ratios. Second, the FLEXPART based results are examined to determine the utility of NMHC ratios as photochemical clocks. Eight different NMHC ratios that are sensitive to the timescales of regional (≈0.3–4 days) and intercontinental (≈4–30 days) transport are considered. These NMHC ratios are formed from the NMHC listed in Table 1. Section 2 discusses the measurements and their analysis; section 3 develops the method for using the FLEXPART results to analyze the interaction of mixing and aging during transport; section 4 compares the FLEXPART analysis to the measurements; and section 5 discusses the results. An important conclusion is that NMHC ratios are useful not only as photochemical clocks to follow photochemical processing but also their interrelationships provide useful diagnostics of the treatment of mixing and photochemical aging in chemical transport models.

2. Data Sets and Analysis Methods

[6] Three different research groups collected the NMHC data included in this paper. The NOAA WP-3D aircraft collected canisters during ITCT 2K2 and ICARTT; these canisters were returned to the laboratory for analysis [*Schauffler et al.*, 1999, 2003]. The NASA DC-8 aircraft also collected canisters during ICARTT, which were analyzed at a different laboratory [*Blake et al.*, 2003]. During NEAQS 2002 and 2004 NMHC were measured by an online, automated GC-MS instrument [*Goldan et al.*, 2004] that was deployed on the NOAA Research Vessel *Ronald H. Brown*, which cruised along the U.S. east coast

Table 1. Kinetic and Emission Ratio Data for Nonmethane Hydrocarbons (NMHCs)

NMHC	OH Rate Constant,[a] 10^{-12} cm^3 molec^{-1} s^{-1}	Molar Emission Ratio[b]
Ethane (C_2H_6)	0.18	1
Propane (C_3H_8)	0.89	0.63
n-butane (C_4H_{10})	2.05	0.35
i-pentane (C_5H_{12})	3.6	0.554
n-hexane (C_4H_{10})	5.2	0.064
Benzene (C_6H_6)	1.22	0.077
Toluene (C_7H_8)	5.63	0.289
o-xylene (C_8H_{10})	13.6	0.049
1,2,4-trimethylbenzene (C_9H_{12})	32.5	0.047

[a]Rate constant data from *Atkinson and Arey* [2003] with T = 273 K for the alkanes and T = 298 K for the aromatics.

[b]Alkane emission ratios through n-butane are the average of the results from *Goldstein et al.* [1995] and *Swanson et al.* [2003]; heavier alkane and aromatic emission ratios are from the results of *de Gouw et al.* [2005].

and concentrated in the Gulf of Maine [*Warneke et al.*, 2004]. All of the analysis systems were calibrated using numerous gas standards.

[7] The accuracy and precision of NMHC measurements in field studies are not well defined, since no formal intercomparison of ambient measurements in nonurban environments has been reported. Nominal reported accuracies and precisions are, e.g., ±5% and the larger of ±1% or 2 pptv, respectively, for the PEM West B study [*Hoell et al.*, 1997]. During ICARTT three intercomparison flights were conducted between the NOAA WP-3D and the NASA DC-8 aircraft. The results of these comparisons suggest a nominal overall uncertainty of 5% + 1 pptv is a reasonable estimate. In the analysis that follows, this value is taken as the 1-sigma confidence limit for each NMHC measurement. This confidence limit is included in error propagation treatments for weighting linear, least squares fits, and used to assign confidence limits to derived parameters. This same confidence limit is assigned both to the NMHC measurements and to the NMHC levels derived from the FLEXPART calculations.

[8] Lower limits are applied to both the measured and the FLEXPART derived NMHC levels. The DC-8 data set does not report measurements below 3 pptv. In the other two aircraft data sets and the ship data set reported NMHC measurements below 1 pptv are not considered. The same lower limits are applied to the NMHC levels derived from FLEXPART for the respective data sets. These limits minimize the scatter in the measured NMHC ratios that result when the ambient concentrations approach the instrumental detection limits and ensure that the measured and modeled NMHC ratios are appropriately compared.

[9] The following analysis relies on linear, least squares regressions between the natural logarithms of NMHC ratios. A weighted regression that allows for uncertainties in both the x and y variables [*Neri et al.*, 1989; *Press et al.*, 1992] is utilized. The weighting for each variable is taken as $1/\sigma^2$ where σ is the estimated uncertainty in each variable propagated from the 1-sigma confidence limits discussed above.

3. Mixing and Aging Treatment

3.1. Aging in an Isolated Air Parcel

[10] Consideration of the evolution of NMHC concentrations in an air parcel isolated from the effects of emissions and mixing, suggests that measured NMHC ratios should provide useful indicators (i.e., "photochemical clocks") of the degree of photochemical processing in a sampled air parcel. The mathematical treatment below is equivalent to those presented by others [e.g., *Roberts et al.*, 1984; *Rudolph and Johnen*, 1990], but is included here in explicit detail for clarity. The concentration of a particular NMHC, [A], at the time of measurement, t_M, can be expressed from simple chemical kinetic theory;

$$\ln[A] = \ln[A]_0 - \int_{t=t_E}^{t_M} k_A[OH]dt, \tag{1}$$

where $[A]_0$ is the NMHC concentration at the initial emission time, t_E, and k_A is the rate constant for reaction with OH. Equation (1) suggests the physical meaning and an operational definition of what will be called photochemical age, t_a:

$$t_a\langle[OH]\rangle = \int_{t=t_E}^{t_M} [OH]dt = -\frac{1}{\langle k_A\rangle}\ln\left(\frac{[A]}{[A]_0}\right). \tag{2}$$

[11] Equation (2) indicates that the photochemical age is directly proportional to the time integral of the [OH] in the air parcel between emission and measurement, and that it can be calculated from the ratio of the NMHC concentration at emission to that measured later.$\langle[OH]\rangle$ represents the constant, average OH concentration between t_E and t_M, and acts as a proportionality constant in equation (2) to give units of time to t_a. In equation (2) $\langle k_a\rangle$ represents an [OH]-weighted, average rate constant, which is generally a function of the temperature that can vary during the time interval. Simultaneous consideration of two NMHC in an isolated air parcel removes the necessity of knowing the absolute magnitude of the NMHC concentration at the initial emission time. Equation (2) becomes

$$t_a\langle[OH]\rangle = \int_{t=t_E}^{t_M} [OH]dt = -\frac{1}{\langle k_A - k_B\rangle}\left\{\ln\left(\frac{[A]}{[B]}\right) - \ln\left(\frac{[A]_0}{[B]_0}\right)\right\}, \tag{3}$$

where $[A]_0/[B]_0$ is the emission ratio of the two NMHC. Measurement of any two NMHC concentrations will thus provide an estimate of t_a if their emission ratio is known and an estimate of $\langle[OH]\rangle$ is available.

[12] Comparison of estimates of t_a from two different NMHC ratios provides a test of the quantitative utility of such t_a estimates. Applying equation (3) to two different ratios yields

$$\ln\left(\frac{[A]}{[C]}\right) = -\frac{\langle k_A - k_C\rangle}{\langle k_B - k_C\rangle}\ln\left(\frac{[B]}{[C]}\right) + b, \tag{4}$$

where b is a function of the two emission ratios and the three rate constants. Equation (4) indicates that if a data set of NMHC measurements is collected in isolated air parcels, then the natural logs of the two ratios should define a linear

relationship with the slope determined only by the OH rate constants.

[13] Figure 2 presents the comparison suggested by equation (4) for the two NMHC ratios formed from the three least reactive alkanes. Data from the WP-3D and DC-8 aircraft in the 2004 ICARTT study are compared to those collected on the WP-3D in the 2002 ITCT 2K2 study. In Figure 2 (as in all NMHC ratios discussed in this paper) the less reactive NMHC is selected for the ratio denominator so that progressively more aged air parcels exhibit progressively smaller ratios. Several points regarding Figure 2 should be noted.

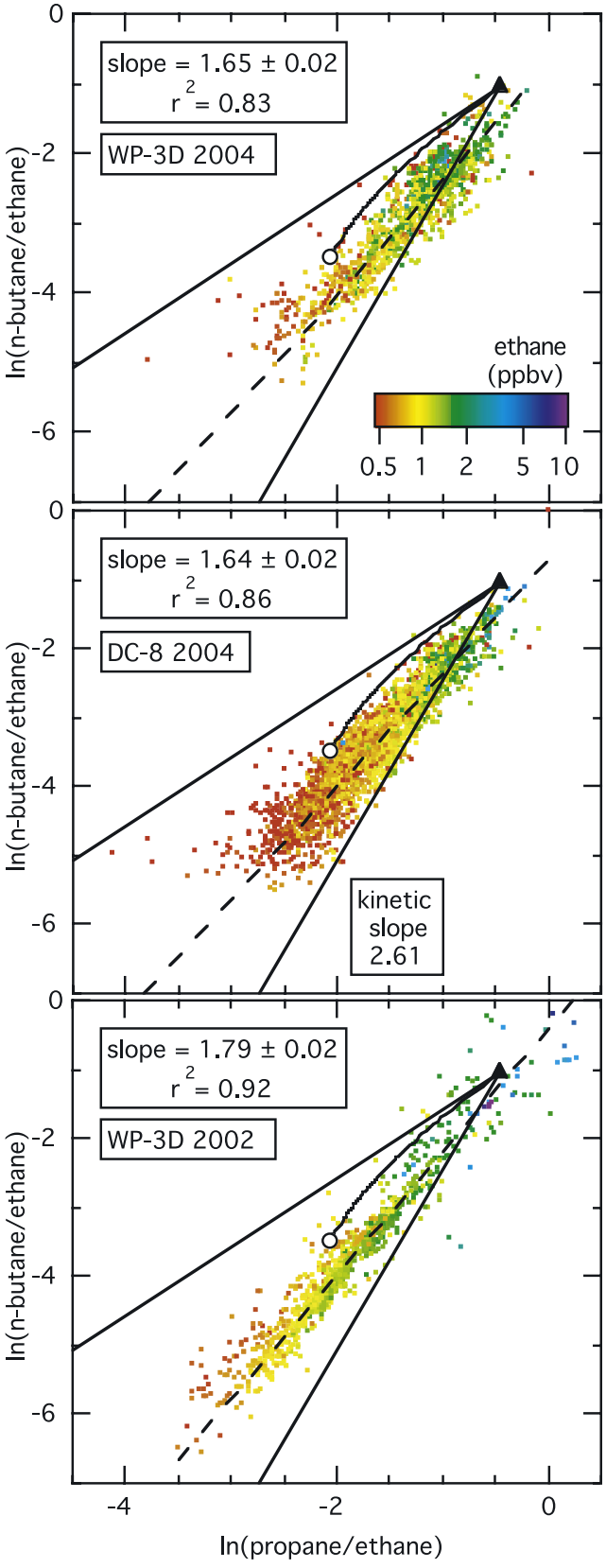

Figure 2. Correlation of the natural logarithms of two alkane concentration ratios for samples collected during three aircraft field studies (dots), color coded according to the log of the ethane concentration. The dashed lines show orthogonal linear least squares fits to the respective data sets, and the slopes with 95% confidence limits and correlation coefficients of those fits are annotated. In each panel the steeper straight solid line indicates aging of an isolated air parcel beginning at the estimated Northern Hemisphere average emission ratio (triangle); the other straight line gives the one-to-one line that limits the effect of mixing. The curved solid line indicates mixing of fresh emissions into the troposphere treated as a well-stirred reactor (circle). See text for more details regarding these lines.

[14] First, lower ethane concentrations generally correlate with lower ratios. This is important, since this is the correlation expected if aging is indeed causing the observed relationships. A certain degree of correlation is expected between these ratios even without aging effects, since the same NMHC is selected for the denominator of both ratios; however if this were the primary cause of the relationship, smaller ratios would correlate with higher ethane concentrations. The observed correlation supports the interpretation of NMHC ratios as measurements of aging.

[15] Second, there is excellent agreement between the NMHC ratio relationships in the 2004 WP-3D and DC-8 data sets; the derived slopes in Figure 2 are statistically equivalent. Different investigators measured the NMHC concentrations with different experimental methods and instrumentation from separate aircraft during very different, independently planned flights over eastern North America and the western North Atlantic. The more aged air parcels and lower ethane level evident in the DC-8 data are due to the generally more remote regions targeted by the INTEX-A/ICARTT study. Clearly, the observed relationship is characteristic of the entire study region, and is not dependent upon the measurement techniques or the particular air masses studied.

[16] Third, there is good agreement of the relationships from the two summertime 2004 data sets with that from the springtime 2002 WP-3D data set collected over the western United States and the eastern North Pacific (Figure 2). This observed relationship also agrees well with a variety of studies conducted throughout the Northern Hemisphere through all seasons (see Table 2). The eleven reported slopes average 1.63 with a standard deviation of 6%. Evidently, the observed relationship is approximately constant, at least over the Northern Hemisphere troposphere.

[17] Fourth, even though the observed relationships agree well with each other, they are quite different from the value expected from equation (4) where the kinetic data of

Table 2. Literature Reports of ln(Butane/Ethane) Versus ln(Propane/Ethane) Linear Relationships

Location, Study	Date	Slope	r^2	Reference
N. and S. Atlantic, Polarstern	1987	1.66 ± 0.10	0.71	*Rudolph and Johnen* [1990]
N. Pacific and N. America	1985–1988	1.47	0.89	*Parrish et al.* [1992]
Boreal Canada, NOWES	1990–1992	1.44	0.92	*Jobson et al.* [1994b]
Arctic Canada, PSE	1992	1.68 ± 0.04	0.95	*Jobson et al.* [1994a]
N. Atlantic, ASTEX/MAGE	1992	1.6	0.72	*Blake et al.* [1996]
N. Pacific, PEM West-B	1994	1.78 ± 0.03	0.93	*Parrish et al.* [2004b]
Summit Greenland	1997–1998	1.58	0.83	*Swanson et al.* [2003]
N. Pacific, TRACE-P	2001	1.61 ± 0.01	0.89	this work
N. Pacific and N. America, ITCT 2K2	2002	1.79 ± 0.02	0.92	this work
N. America and N. Atlantic, ICARTT	2004	1.65 ± 0.02	0.83	this work
N. America and N. Atlantic, INTEX-A	2004	1.64 ± 0.02	0.86	this work

Table 1 predict a slope of 2.61, a value 60% larger than observed. Evidently both of these NMHC ratio "photochemical clocks" do evolve with photochemical processing of an air mass, but they do not quantitatively measure the same photochemical age.

3.2. Interaction of Aging and Mixing Between Air Parcels

[18] Mixing between air parcels has been identified as the cause of the failure of the simple relationship between NMHC concentrations given by equation (4) [e.g., *McKeen et al.*, 1990; *Parrish et al.*, 1992; *McKeen and Liu*, 1993; *McKeen et al.*, 1996; *McKenna*, 1997]. The effects of mixing on the measured NMHC concentration in an air parcel can be treated formally by considering a continuous, variable emission flux, $[A]'(t_E)$, into a final sampled air parcel:

$$[A] = \int_{t_E=0}^{t_E=t_M} [A]'(t_E)dt_E. \quad (5)$$

[19] Here each differential emission, $[A]'(t_E)dt_E$, has its own, well-defined emission time, t_E. and represents the concentration of the NMHC that was emitted at time t_E and remains in the air parcel when sampled at time t_M. The integral accounts for emissions from the distant past ($t_E = 0$) up to the measurement time; this integral must be evaluated over many lifetimes of the least reactive NMHC of interest so that [A] at t = 0 can be set to 0. Equation (1) can be applied to give

$$[A]'(t_E) = [A]_0'(t_E) \exp\left\{ - \int_{t=t_E}^{t_M} k_A[OH]dt \right\}, \quad (6)$$

where $[A]_0'(t_E)dt_E$ represents the concentration emitted at time t_E that would remain in the air parcel if it were a nonreactive, conserved tracer.

[20] The treatment outlined in equations (5) and (6) is similar to that applied by others to the interaction of mixing and decay in the atmosphere [e.g., *Brost and Heimann*, 1991; *Kleinman et al.*, 2003] and in the oceans [e.g., *Broecker and Peng*, 1982]. These studies conceptualize an air parcel ensemble model that treats any sampled air parcel as a summation of many discrete parcels, each carrying emissions released at a specific time. The treatment here includes a temporal integration over differential emission elements (equation (5)). Each emission element has a discrete time of emission, and the integration covers the time interval from the distant past (at least many lifetimes of each NMHC of interest) up to the time of measurement. Each emission element is assumed to include all emissions in the entire spatial domain of interest that are mixed and transported into the measured air parcel at the time of sampling.

[21] In principle a hemisphere scale chemical transport model is required for the solution of equations (5) and (6) for any specific sampled air parcel. Our purpose here is to investigate the interaction of aging and mixing on the ratios of NMHC. For this, a model that decouples chemistry from a sophisticated treatment of transport is suitable. Here we use the FLEXPART model calculations to treat transport, and assume constant OH concentrations throughout the troposphere to treat the chemistry. Since we are interested only in NMHC ratios and the chemistry of each NMHC is taken to be first-order loss by reaction with OH, this decoupling provides a useful description of the interaction of aging and the mixing of air parcels of different histories caused by the transport processes in the troposphere. FLEXPART treats these transport processes in as sophisticated a manner as the state of the science presently allows.

3.3. FLEXPART Age Spectra

[22] Here we will use FLEXPART CO emission age spectra [*Stohl et al.*, 2003] as an approximate tool to evaluate the age spectra of NMHC. This approach provides a powerful, albeit limited, technique for the evaluation of equation (6). The CO age spectra were derived from backward simulations, which trace back in time a sampled volume of air and calculate a sensitivity function to emission input [*Stohl et al.*, 2003]. Because of the combined effects of resolved transport and turbulence, the originally (i.e., at the time of sampling) well-defined volume of air quickly becomes dispersed, both horizontally and vertically, and, thus, emissions from large areas can influence a single measurement. By folding (i.e., multiplying) the emission sensitivity function with the CO emission fluxes from an emission inventory, source contribution maps are derived. Figure 3a illustrates one such source contribution map integrated over 20 days of transport where many of the major U.S. urban areas are identifiable. Since the emission sensitivities are stored at daily intervals, source contribution maps can also be calculated every day back in time from the measurement location. Spatial integration of the daily emission contributions then gives the total CO concentration emitted on the corresponding day that is transported and

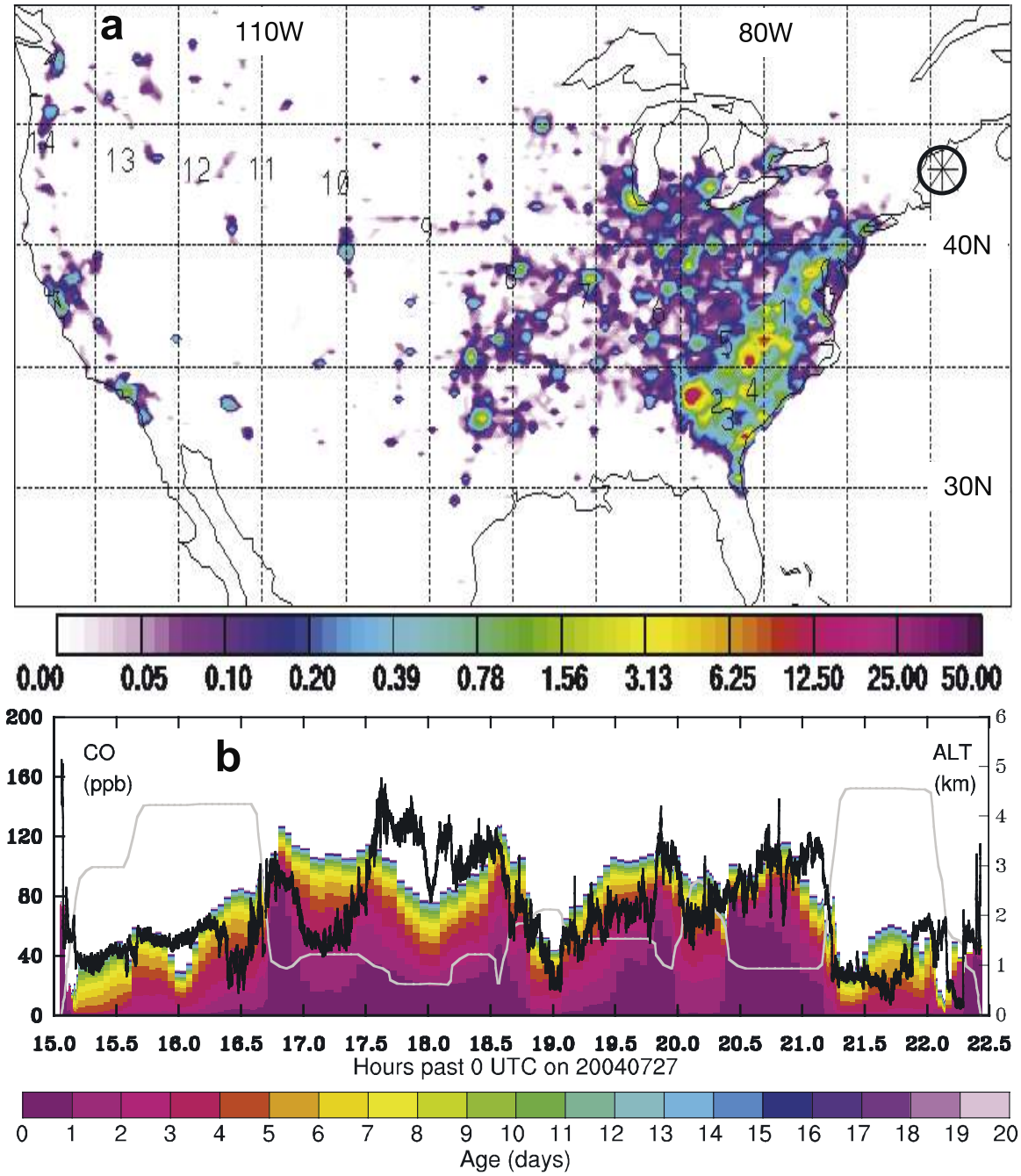

Figure 3. Example results for CO emissions calculated by the FLEXPART Lagrangian particle dispersion model. (a) Map of emission sources for an air parcel intercepted by the WP-3D aircraft at the location marked by the circled asterisk off the coast of Maine. The color coding indicates the emission intensity in units of 10^{-10} ppbv m^{-2}. The numbers on the map give the centroid position of the sampled air mass at daily intervals. (b) Age spectra (colored vertical bars) presented as cumulative histograms for segments of the 27 July WP-3D flight compared to the measured CO concentration (black line). The CO concentration is offset by −60 ppbv to approximately account for the CO background not calculated by FLEXPART. The grey line indicates the flight altitude profile. The color of each age spectrum segment indicates the age of the emissions at the flight intercept time.

mixed into the sampled air parcel. The concentrations from each of the 20 days of calculation constitute the emission age spectrum for the sampled air parcel. Figure 3b shows all of the age spectra (presented as cumulative histograms) calculated for one flight of the NOAA WP-3D aircraft. In essence FLEXPART calculates the surface CO emissions (treated as an inert species) that accumulated in a volume of air as it was transported to the point where it was sampled.

[23] Figure 3b compares the measured CO concentration (offset by −60 ppbv to approximately account for the

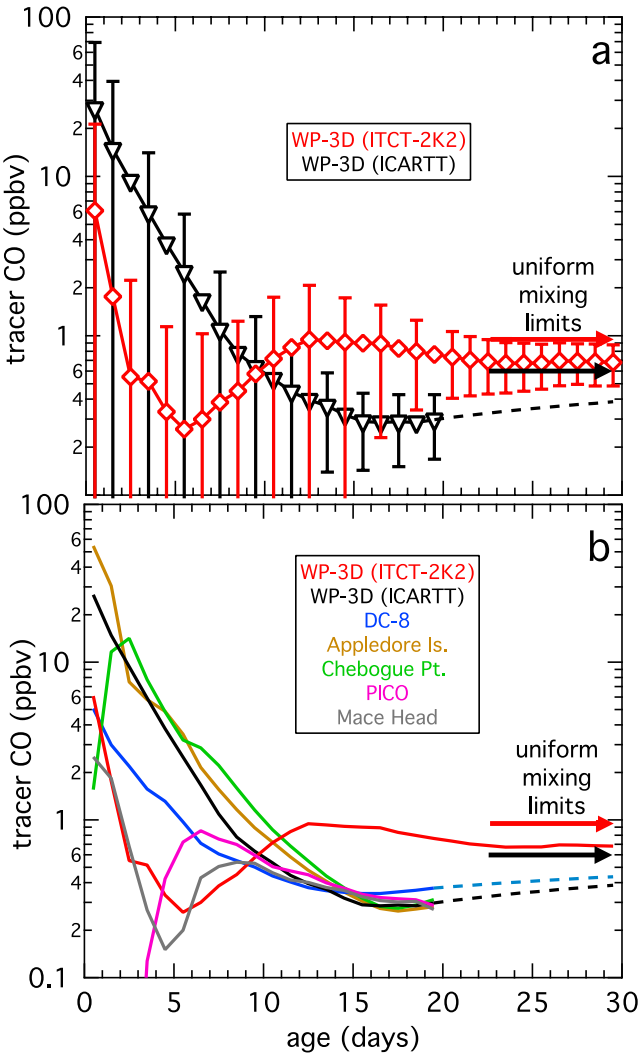

Figure 4. Average age spectra calculated by the FLEXPART Lagrangian particle dispersion model for the indicated platforms and surface sites. (a) Comparison for the WP-3D flights on the western coast (ITCT 2K2) and eastern coast (ICARTT) of North America. The error bars indicate standard deviations of histogram increments. (b) Comparison for seven sites and platforms from the ICARTT study. The dashed lines in the graphs show the average age spectra extrapolated to times longer than those included in the FLEXPART calculations. The two arrows indicate the uniform mixing limits for the WP-3D FLEXPART results discussed in the text.

hemispheric CO background that FLEXPART does not treat) to the upper limit of the cumulative age spectra, which represent the model calculated CO concentration. Generally, the calculated CO levels are comparable to the CO levels encountered in the flight, but transported plumes of North American CO were encountered at locations displaced, particularly in the vertical, from the model calculated locations. Such displacements are common in modeled transport, particularly over oceanic regions where meteorological soundings are sparse.

[24] The FLEXPART model was utilized to calculate age spectra for the ITCT 2K2 and the ICARTT studies. FLEXPART is a Lagrangian particle dispersion model that treats time/space interpolations through coarse-resolution meteorological fields and includes parameterized treatments of convection and turbulent mixing processes [*Stohl et al.*, 2005]. The calculations included here utilized 1° × 1° European Centre for Medium-Range Weather Forecasts (ECMWF) data fields with 60 vertical levels and a temporal resolution of 3 hours. These data were enhanced for the ICARRT study by 0.36° × 0.36° data for a large domain centered over North America and the North Atlantic. The turbulence parameterization was used for both field studies, but the convection parameterization was used only for the ICARTT calculations.

[25] The ITCT 2K2 study in 2002 [*Forster et al.*, 2004] included the total global anthropogenic (Asia, Europe, North America, South America, Africa, and Australia) CO emissions from the EDGAR 1995 emission inventory (file name: ant95co.1 × 1), which also included some biomass burning emissions. The total emissions were 846 Tg/year. The sampled air was followed back for 30 days before it was removed from the calculation. For the ICARTT study in 2004, total global CO emissions were included from the EDGAR 1995 emission inventory with some modifications. Only the EDGAR source categories for non-biomass-burning were included, and for the North America study region an inventory valid for 1999 [*Frost et al.*, 2006] was substituted for the EDGAR emissions. The total emissions were 544 Tg/year. The sampled air was followed back for only 20 days before it was removed from the calculation. For each study, the particles representing the emissions were emitted semicontinuously (every 15 min).

[26] Figure 4 shows the average of all of the age spectra calculated for each of several sampling platforms and surface sites. (Each symbol represents the average and standard deviation of the CO concentration of the indicated age in the air parcels sampled by a given platform or site.) These age spectra represent the air parcels either encountered on segments spaced along the paths traveled by the mobile platforms (see Figure 3b for example), or received at equally spaced time intervals by the surface stations. The number of spectra calculated range from 373 at some of the surface sites to over 8200 for one of the aircraft platforms. Most of the average spectra have maximum emission contributions on the first day, which reflects the importance of fresh, concentrated emission plumes, even for the aircraft platforms. However, the two more remote surface sites (Chebogue Point in Nova Scotia, and PICO in the Azores) have maximum emission contributions at later times (3rd and 7th day, respectively) indicating the most probable transport times of continental emissions to these sites. The average age spectra for Mace Head, located on the west coast of Europe, and for the WP-3D ITCT 2K2, operated on the west coast of North America, both show secondary maxima, which represent transport from the upwind continent. The times of these secondary maxima, 9 and 13 days, represent the most probable times for transatlantic and transpacific transport of the continental emissions during the seasons of the respective studies. These times are consistent with the results of *Stohl et al.* [2002].

[27] Interestingly, in Figure 4 the average spectra each converge to a limit, with smaller variation about the average, at the later days. This feature is particularly clearly defined

for the ITCT 2K2 calculation that extends to 30 days. The convergence limits agree reasonably well with the uniform mixing limits (indicated by the arrows in both panels of Figure 4), which correspond to the total global anthropogenic CO emissions per day dispersed throughout the troposphere of the Northern Hemisphere. This approximation is appropriate since only a small fraction of the global anthropogenic emissions are released in the Southern Hemisphere. The time required for complete dispersion of emissions from their predominately midlatitude source regions throughout the Northern Hemisphere troposphere is likely longer than the 20 or 30 days covered by the FLEXPART calculation. Since the measurements were predominately localized in the midlatitudes as well, the enhanced concentration of the emissions in the measurement region approximately compensates for the fraction of the emissions released in the Southern Hemisphere. The different limits for the 2002 and the 2004 studies result from the different emission inventories used in the FLEXPART calculations for the two years.

[28] For each NMHC of interest in a given air parcel, the integral of equation (5) is evaluated through summation of the concentration increments contributed by each day of the corresponding age spectrum. Each concentration increment is derived from equation (6) through several simplifying assumptions. $[A]_0(t_E)$ for each NMHC is taken as proportional to the CO emissions. The integral in equation (6) is evaluated by assuming constant [OH], which is set equal to a nominal value for the diurnally averaged, regional hydroxyl radical concentration, and temperature-independent rate constants. Table 1 summarizes the required NMHC emission ratios and kinetic rate constants.

[29] The NMHC emissions are derived from the CO emissions by multiplying by the ethane to CO molar emission ratio, estimated as 0.0114, and by the NMHC emissions relative to ethane included in Table 1. The CO to ethane molar emission ratio value is the average from two recent inventories: the POET 2000 (http://www.aero.jussieu.fr/projet/ACCENT/POET.php) ratio of 0.0092 and the RETRO 2000 (http://www.retro.enes.org/emissions/) ratio of 0.0135. These ratios, as well as the CO emission inventory used in the ICARTT FLEXPART calculations, exclude biomass burning emissions. This is appropriate since the ambient data sets considered are dominated by anthropogenic emissions of both CO and NMHC.

[30] The first-order decay of NMHC through reaction with OH described in equation (6) is approximately evaluated as appropriate for the season of the study and the likely temperature field encountered by the respective NMHC during aging. The diurnally averaged regional hydroxyl radical concentrations are set equal to 1×10^6 cm^{-3} for the springtime ITCT 2K2 study and 2×10^6 cm^{-3} for the other, all summertime data sets. These values are in approximate accord with model studies [e.g., *Spivakovsky et al.*, 2000]. The rate constants for the slower reacting alkanes correspond to 273 K, a temperature representative of the free troposphere since these NMHC live long enough to be widely dispersed. The rate constants for the faster reacting aromatics correspond to 298 K, a temperature representative of the boundary layer where those NMHC are primarily emitted and react before they can be widely dispersed. The ratios of these rate constants, particularly for the aromatics, are not strongly dependent upon temperature.

[31] The evaluation of equation (5) requires integration of the NMHC accumulated in the air parcel from the distant past ($t_E = 0$) up to the time of measurement. The last 20 or 30 days before measurement are evaluated from the corresponding FLEXPART age spectrum. These spectra were archived with a 1-day temporal resolution. This resolution is not adequate for the treatment of rapidly reacting NMHC, so the results are dependent upon how each day's emissions are apportioned over the 24-hour period. Here for each histogram we randomly select a specific time within each histogram increment, and assume that the day's NMHC emissions were all released at that time. This approach gives a full range of NMHC processing times including nearly fresh emissions; the results are not markedly different from those obtained by assigning each day's emissions to the center of the 24-hour period, except that in our selected approach unprocessed emissions of the rapidly reacting NMHC are represented. The effect of the random emission time assignment within a 24-hour period is inconsequential, since in either case the interrelationship of the diurnal variation of [OH] with the emission and sampling times in the integral of equation (6) is neglected.

[32] For longer-lived NMHC accurate evaluation of equation (5) requires integration to emission times earlier than the 20 or 30-day periods covered by the FLEXPART age spectra. This integration is accomplished by extrapolating each age spectrum indefinitely back in time. In the selected extrapolation the average emission increment of the last day of the FLEXPART calculation is exponentially relaxed to the corresponding uniform mixing limit. A 30 day relaxation time is selected, which conceptually corresponds to the approximate time constant for dispersion of an emission pulse throughout the Northern Hemisphere troposphere. Once this extrapolation begins, all age spectra for a given site or platform are identical. The arrows in both panels of Figure 4 show these extrapolations of the age spectra for two platforms.

[33] It should be noted that the approach outlined above will limit the final results to a statistical comparison of the NMHC ratios calculated from the FLEXPART age spectra to those measured; it will not allow a one-to-one comparison of the ratios measured in a particular NMHC sample to those calculated from the corresponding age spectrum. Any one-to-one comparison would be compromised by the assumption of a constant [OH] in the FLEXPART based model while the measurements reflect emissions that in reality have been processed by [OH] that varies from essentially zero at night to nearly an order of magnitude larger than [OH] during peak photochemical activity.

3.4. Heuristic Models

[34] There are three simple heuristic models of the interaction of aging and mixing that are useful to consider; they define the black symbols and solid black lines included in Figure 2. The triangle indicates fresh emissions according to the emission ratios of Table 2. The first heuristic model ignores mixing effects and uses equation (4) to calculate the evolution of those initial NMHC ratios; that result is indicated by the steeper solid line whose slope is indicated in Figure 2. The second model ignores aging and assumes that the fresh emissions simply mix into background air that is so well aged that only the least reactive NMHC remains at

significant concentrations. That mixing causes the fresh emission ratios to decrease with a slope of unity, and is indicated by the less steep solid line. The third model assumes that the troposphere behaves like a well-stirred reactor; that is, mixing of fresh emissions into the background air is complete before reaction proceeds to a significant extent, and that the first-order removal of the NMHC takes place in a uniform, well-mixed troposphere. The NMHC ratios in that uniform mixture are defined by

$$\frac{[A]}{[B]} = \frac{E_A k_B}{E_B k_A}, \tag{7}$$

which is given by the circle in Figure 2; E_A is the molar emission ratio of NMHC A to ethane given in Table 1. The curved solid line that connects the triangle and the circle is the mixing curve defined by fresh emissions dispersing into the well-stirred equilibrium mixture.

[35] The ratios derived from the ambient measurements in Figure 2 are generally confined between the two solid straight lines. The data outside this segment of the graph appear to be dominated by fresh emissions with emission ratios systematically different from those assumed (Table 1), and with significant variability. It must be remembered that the assumed emission ratios are derived from studies reported in the literature; evidently the emissions that dominate the 2004 study region (northeastern North America) are not well characterized by global average emission ratios. The linear–least squares fit to the ambient data for the two 2004 data sets fall below the fresh emission point, and are in excellent agreement with each other, which indicates that the fresh northeast U.S. emissions sampled in this study are enriched in propane relative to n-butane when compared to the global average. The fresh emissions in the region of the 2002 study are more closely in agreement with the global averages. Indeed, it is the disagreement in the fresh emission ratios that largely account for the difference in slope between the east and west U.S. coast studies; the data points at the more aged end of the distributions generally overlap quite well in all three studies of Figure 2.

[36] The enrichment of propane in the fresh emissions of the 2004 study region is supported by the shipboard measurements made both in NEAQS 2002 [*de Gouw et al.*, 2005] and 2004 (C. Warneke et al., Measurements of urban VOC emissions ratios and comparison with inventories, manuscript in preparation, 2007) in the ICARTT study region. Those two studies found average propane to n-butane emission ratios of 3.8 and 4.5, respectively, which are a factor of 2 to 3 larger than the emission ratio of 1.8 from Table 1. Plots analogous to Figure 2 for these two studies exhibit quite shallow slopes (0.97 and 1.08, respectively), which result from the contrast of the propane-enhanced fresh emissions with aged air parcels transported from regions with more typical emission ratios.

[37] In Figure 2 very few of the ambient data lie above the result from the well-stirred reactor model. This is perhaps not surprising, since it is quite extreme to envision that mixing and dispersion throughout the troposphere proceed much faster than NMHC removal by reaction with OH. However, the age spectrum associated with this well-stirred reactor assumption is simply a uniform histogram with all days having a contribution equal to the uniform mixing limit illustrated in Figure 4. It is possible to imagine a bimodal age spectrum that would give a result that falls above the well-stirred reactor limit. Indeed, the age spectrum that corresponds to fresh emissions mixing into very well aged air (the upper straight line with a slope of unity in Figure 2) is a sharp peak at very short times, and a peak at times old enough that the more reactive NMHC are reduced to insignificant levels. Age spectra with varying relative sizes of these peaks would trace out that upper straight line.

4. Results

4.1. Light Alkane Ratios

[38] Figure 5 shows the modeled results for the relationship between the two NMHC ratios formed from the three least reactive alkanes. Each point is derived from one of the FLEXPART age spectra as outlined in section 3.3. The FLEXPART relationships for the three data sets in Figure 5 give a good representation of the measurements in Figure 2. Figures 2 and 5 are in the same format to allow direct comparisons between the measurements and model results. The model slopes agree well with those measured in all cases (4 to 8% high), and all modeled slopes are well below the kinetic limit. The measurements and model agree that the WP-3D, on average, observed more aged NMHCs coming ashore on the U.S. west coast from the Pacific Ocean during 2002, than leaving the east coast during 2004. Evidently the dispersion and mixing treatment included in the FLEXPART analysis is adequate to describe the primary mixing effects apparent in the relationships of the measured NMHC ratios.

[39] The ranges of the NMHC ratios are similar in the model and the measurements for each of the three studies; however, these ranges are partially dependent upon the lower limits of the NMHC concentrations included in the measurements and in the model results. The two WP-3D measurement sets had no measurements with any of the three NMHC below the detection limit (1 pptv), although that limit was approached or reached in both studies. The FLEXPART calculations predict, however, that about 4% (Table 3) of the n-butane measurements would have been below the detection limit for both WP-3D studies. The results for these air parcels have been removed from the plots in Figure 5. This difference between the measured and modeled NMHC distributions may reflect the sampling strategy on the WP-3D aircraft, where the samples were predominately collected in emission plumes. In contrast, the DC-8 data set reported 11% of the n-butane measurements below the detection limit (3 pptv), while FLEXPART results predict that 47% of the measurements would be below that limit. This difference may indicate that FLEXPART underestimates the quantities of NMHC emissions dispersed into the more remote air masses targeted by the DC-8; a possible reason for such an underestimate is the large impact of convection, which was particularly important during the 2004 ICARTT study. The difference in percentage of points below the detection limit could also result from a smaller average OH concentration experienced by the air parcels sampled by the DC-8 compared to the WP-3D samples.

[40] The FLEXPART age spectra treatment in section 3.3 was intended only to model NMHC ratios, but the applica-

tion of that treatment requires the calculation of absolute NMHC concentrations from which the ratios are calculated. These absolute concentrations are not necessarily expected to accurately represent the real atmosphere. Nevertheless the calculated ethane levels are not unreasonable as indicated by the color scales in Figure 2. Note however, that the color scales are approximately a factor of 2 different; this change was made in Figure 5 to improve the agreement of colors with Figure 2. Adjustment of the assumed total CO emissions, assumed ethane to CO emission ratio, and/or the assumed OH concentration would improve the agreement between measurements and model without strongly affecting the derived slopes, but such tuning is not expected to lead to useful conclusions. It should be noted that the derived slopes in Figure 5 are not strong functions of the assumed OH concentration, although the absolute concentrations are quite sensitive.

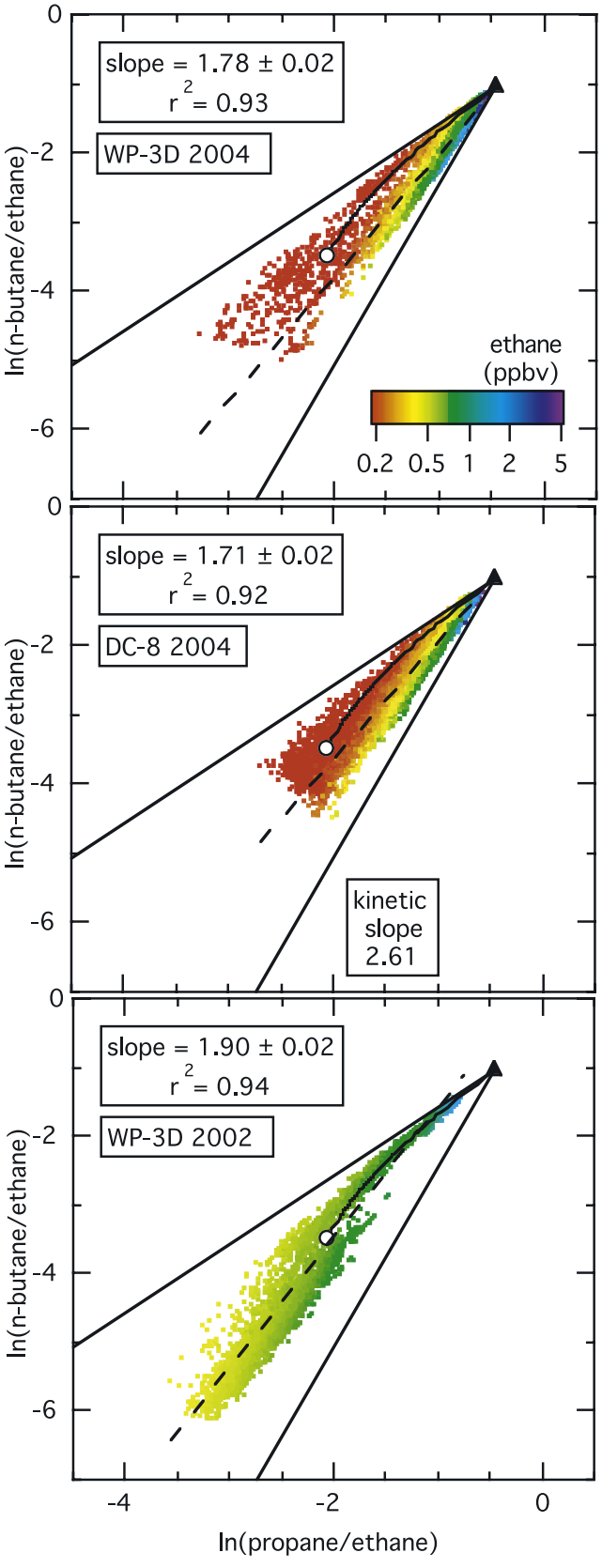

[41] It is interesting to note in Figure 5 that for two air parcels with the same value for one of the NMHC ratios, the parcel with the higher ethane concentration generally falls closer to the steeper kinetic line. The measurements in Figure 2 show this same behavior, although certainly less clearly. The likely explanation for this feature is as follows. In an aged air parcel with high ethane concentration, the NMHC generally have been dominated by a single large injection of emissions; mixing effects are then much smaller and more nearly kinetic behavior is exhibited. In a similarly aged parcel with low ethane concentrations, multiple small injections of NMHC emissions have been mixed to yield the average age and the low ethane concentrations.

4.2. Interpretation of Photochemical Age

[42] If a given air parcel contains species emitted at different times, then the concept of the age of that air parcel, or more explicitly the age of the emissions in that air parcel, is not well defined. From any particular measured hydrocarbon ratio, a photochemical age can be calculated from equation (3), but each hydrocarbon ratio is likely to give a different value for the photochemical age, so the interpretation of photochemical age as discussed in section 3.1 is also not well defined. However, it is possible to define the average age of each particular hydrocarbon in any air parcel, which then is well defined; it is the concentration-weighted average age of the hydrocarbon emissions that have accumulated in that air parcel through all emission and mixing processes. It is given by

$$\langle age \rangle = \int_{t_E=0}^{t_E=t_M} (t_M - t_E)[A](t_E)dt_E \Big/ [A], \qquad (8)$$

and can be calculated from a FLEXPART age spectrum much as the hydrocarbon ratios were calculated in section 3.3. Figure 6 compares ⟨age⟩ (equation (8)) for five alkanes to the photochemical age (equation (3)) based on the n-butane/ethane ratio. These calculations have been

Figure 5. Correlation of the natural logarithms of two alkane concentration ratios calculated from FLEXPART age spectra for three aircraft field studies (dots) in the same format as Figure 2. The dashed lines show orthogonal linear least squares fits to the respective studies, and the slopes with 95% confidence limits and correlation coefficients of those fits are annotated. The solid lines and symbols give limiting behavior discussed in the text.

Table 3. Percent of NMHC Ratios With Either NMHC Below the Instrumental Detection Limit[a]

Platform	n-Butane/Ethane	i-Pentane/Propane	o-Xylene/Benzene	Trimetylbenzene/Toluene
WP-3D 2004 exp[c]	0	3.3	40	52
WP-3D 2004 FLEX[d]	4.5	6.1	42	70
DC-8 2004 exp[c]	11	38	92	98
DC-8 2004 FLEX[d]	4.6	53	90	96
WP-3D 2002 exp[c]	0	2.7	...	...
WP-3D 2002 FLEX[d]	3.5	27	76	83
RHB[b] 2002 exp[c]	0.5	4.7	15	16
RHB[b] 2002 FLEX[d]	...	...	...	...

[a]The detection limit is taken as 1 pptv for the WP-3D and RHB data sets and 3 pptv for the DC-8 data set (see section 2 for more discussion).
[b]RHB represents *Ronald H. Brown* Research Vessel.
[c]exp represents measured data set.
[d]FLEX represents the results from the age spectra calculations.

done for the FLEXPART age spectra from the WP-3D 2002 study, and the photochemical age in units of days is obtained by dividing the left side of equation (3) by $\langle[OH]\rangle$ set equal to 1×10^6 cm^{-3}.

[43] Figure 6 shows that, although the average age of each alkane correlates reasonably well with the photochemical age, there is a large difference in the average ages of the five alkanes at a given photochemical age, and that there is no alkane with an average age equal to the photochemical age at all times. This difference is as expected since longer-lived alkanes have older average ages in mixtures of alkanes emitted over a period of time. In Figure 6, it is clear that the average age of the alkane (propane) that has a rate constant between the rate constants of the alkanes (ethane and n-butane) on which the photochemical clock is based is most accurately represented by the photochemical age; *Parrish et al.* [1992] and *de Gouw et al.* [2005] reached similar conclusions. As the rate constant of the alkane increases further above the rate constants of those in the photochemical clock ratio, the correlation between the average age and the photochemical age worsens. In summary, the average age of a NMHC can be approximated well by the photochemical age based upon a properly chosen HC ratio, and there is a correlation between the photochemical age and the average age of any NMHC, but that correlation worsens as the rate constants become more disparate. The approximations and correlations will be better in air parcels where the concentrations of the species of interest were all injected in a narrow period of time in the past; that is, the age spectra are sharply peaked.

4.3. C_3–C_5 Alkane Ratios

[44] Ratios of faster reacting NMHC are better suited to follow transport and mixing processes that occur on timescales shorter than tens of days as is the case (Figure 6) for the ratios from the C_2–C_4 alkanes. In this section we examine the evolution of the ratios of a C_4 and a C_5 alkane to propane. Propane rather than ethane is selected for the denominator, since alkanes of similar masses generally are emitted by similar sources, which reduces the scatter resulting from variation in the NMHC emission ratios. The C_5 alkane selected is i-pentane rather than the normal isomer because it is generally more abundant in anthropogenic emissions.

[45] Figure 7 shows the correlation between two NMHC ratios for the same field studies and in the same format as Figure 2 for the lighter NMHC ratios. The features of Figure 7 are qualitatively similar to Figure 2, but there are

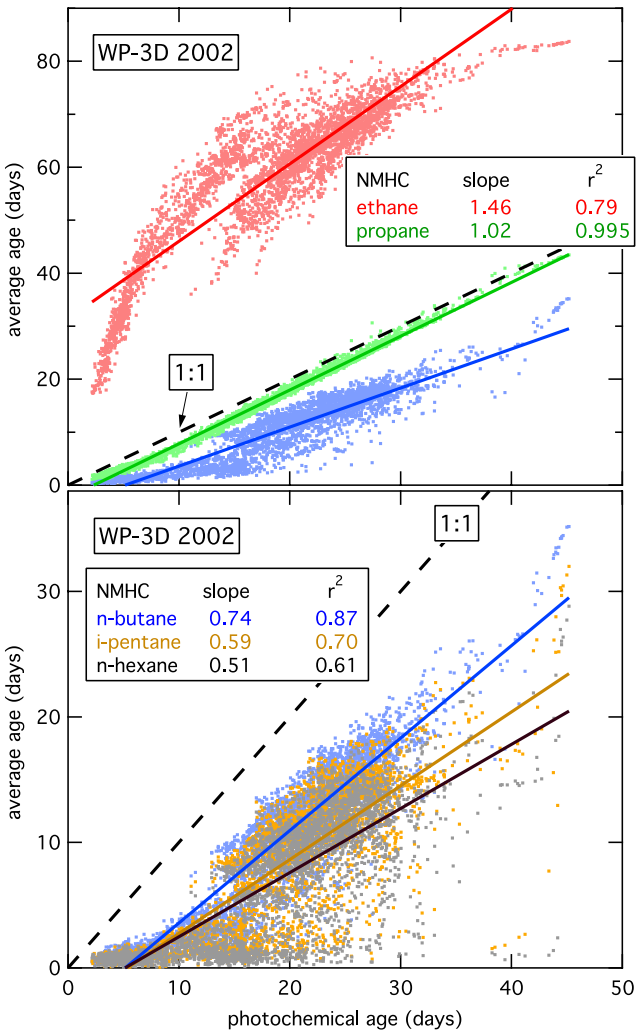

Figure 6. Correlations between the average ages of five alkanes and the photochemical age from the n-butane/ethane ratio. The light-colored dots are derived from the FLEXPART age spectra for the 2002 WP-3D flights. The darker-colored lines indicate standard linear least squares fits to the respective hydrocarbon ages, with the slopes and correlation coefficients of those fits annotated. The n-butane results are included in both figures.

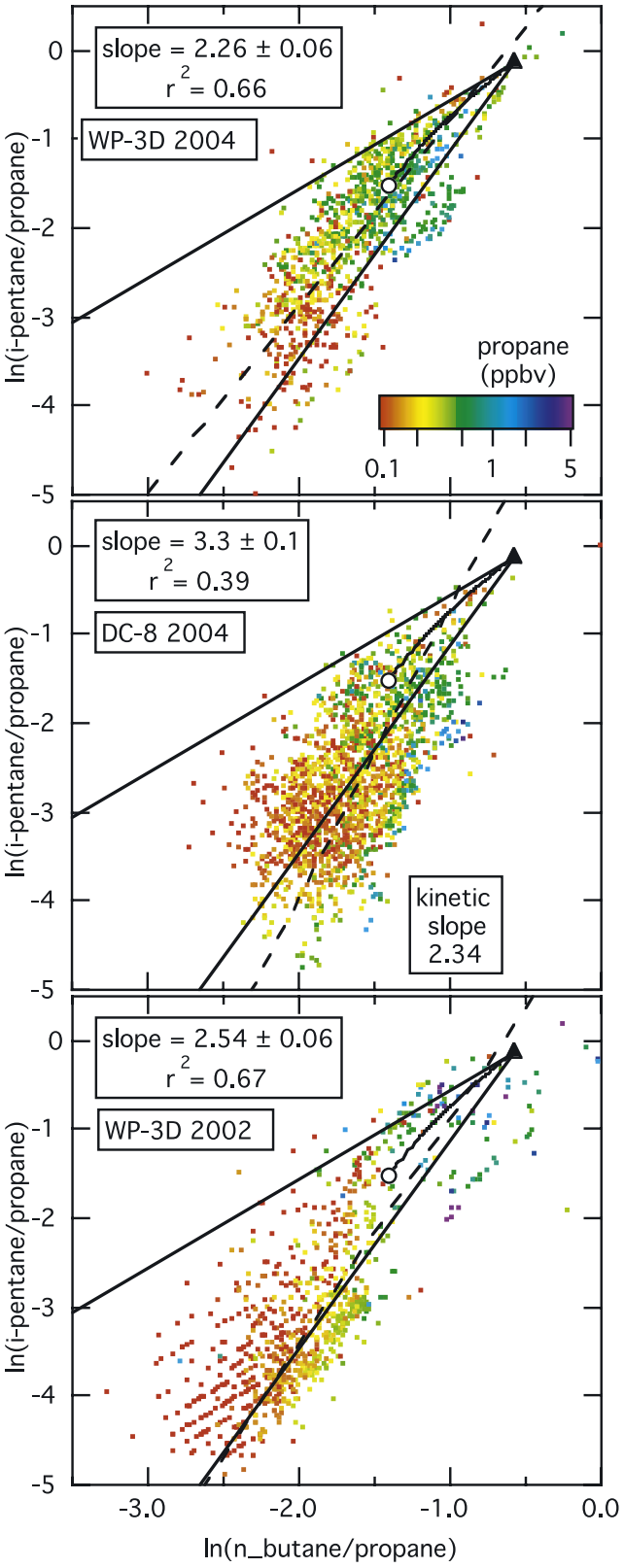

Figure 7. Correlation of the natural logarithms of two alkane concentration ratios for samples collected during three aircraft field studies (dots), color coded according to the log of the propane concentration. The format is the same as in Figure 2. The solid lines and symbols give limiting behavior discussed in the text.

important quantitative differences. Similar to Figure 2, lower propane concentrations generally correlate with smaller ratios, again indicating that aging is indeed causing the observed relationships.

[46] One important difference is that the data in Figure 7 more closely follow the relationship expected from aging in the absence of mixing (i.e., the steeper solid line.) Indeed, the data scatter about that line and the slopes of the relationships from the two WP-3D data sets agree with the slope expected from the kinetic rate constants of Table 1 to within ±9%.

[47] Another important contrast between Figure 2 and Figure 7 is that the latter shows greater differences between platforms than between field studies, and the correlations are poorer for all three data sets. In Figure 7 the DC-8 2004 data set gives a significantly steeper slope (3.3) than the WP-3D data sets (average of 2.4) or the kinetically expected slope (2.34), and many of the data lie below the steeper solid line. The DC-8 behavior is not consistent with aging and mixing of emissions, at least if emitted with a common emission ratio. This may well indicate experimental problems in determining the very low i-pentane concentrations encountered in the DC-8 2004 flights. During three intercomparison flights in 2004, the DC-8 reported i-pentane concentrations about a factor of two lower than the WP-3D at levels below about 20 pptv. In Figure 2 the r^2 values lie between 0.83 and 0.92. In Figure 7 the WP-3D r^2 values are both lower at about 0.66,and the DC-8 value is even lower at 0.39, which again emphasizes the experimental difficulties encountered in quantifying NMHC concentrations at low pptv levels.

[48] The FLEXPART results (Figure 8) predict slopes (2.04 to 2.16) that are in near agreement with kinetic behavior (slope of 2.34) in reasonable accord with the experimental data of Figure 7. It should be noted that the linear least squares fits to the FLEXPART results, as well as to the experimental data, are weighted by the measurement precision expected for either the calculated or the measured NMHC concentrations. As a consequence, in the FLEXPART results, the lower concentrations scatter toward the mixing line, and away from both the least squares fit and kinetic line. This behavior is not so apparent in the experimental data except for the WP-3D 2002 data set.

[49] As was found for the light alkanes, the ranges of the NMHC ratios are similar in the model and the measurements for each of the three studies. The two WP-3D measurement sets had about 3% of the measurements with a NMHC below the detection limit (Table 3). The FLEXPART calculations predict that a 2 to 10 times larger fraction of the i-pentane measurements would be below the detection limit for the WP-3D studies. The factor of 10 difference in the WP-3D 2002 data set may reflect underestimates in the emissions of NMHC from Asia, in accord with the underestimates found for CO [*Forster et al.*, 2004]. In contrast, the DC-8 data set with 38% of the i-pentane measurements below the detection limit agrees much better with the FLEXPART results that predict that 53% of the measurements below that limit.

4.4. Aromatic Ratios

[50] The aromatics provide particularly promising NMHC ratios for following photochemical processing on timescales

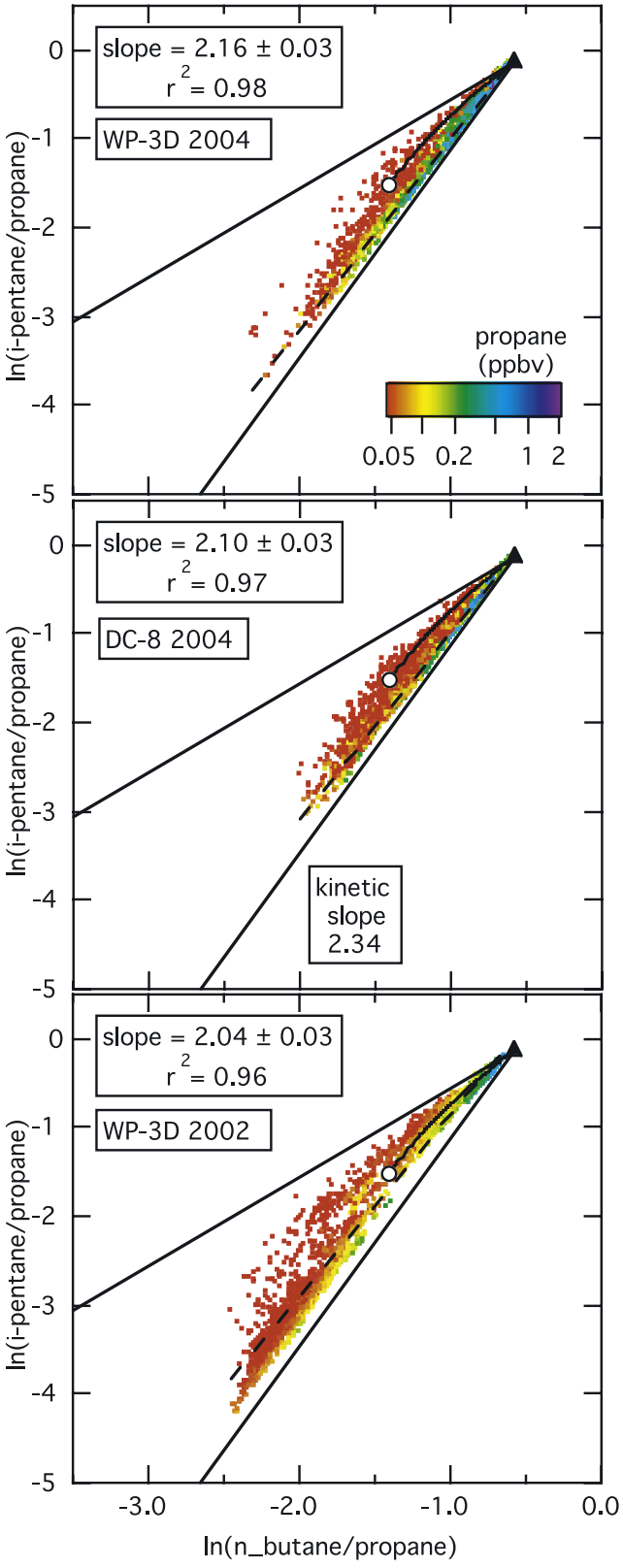

Figure 8. Correlation of the natural logarithms of two alkane concentration ratios calculated from FLEXPART age spectra for three aircraft field studies (dots) in the same format as Figure 7.

of hours to days [e.g., *de Gouw et al.*, 2005]. Figures 9–12 present the correlations between two different pairs of NMHC ratios derived from 4 aromatics that span a wide range of lifetimes (Figure 1). Figures 9 and 11 include the experimental correlation from the 2002 *Ronald H. Brown* shipboard measurements of the NEAQS study with the correlations from the two 2004 aircraft data sets from previous figures. (The 2002 WP-3D study did not measure the more reactive aromatic, and the 2004 *Ronald H. Brown* measurements include some anomalous results that deviate from the other data sets.) Figures 10 and 12 present the corresponding results from the FLEXPART based calculations. (FLEXPART calculations were not performed for the NEAQS 2002 study.)

[51] Figure 9 and 10 indicate a striking contrast between the measurement and model behavior for ratios with benzene in the denominator. Three different laboratories using different experimental techniques from three different platforms made the measurements in Figure 9, yet they agree reasonably well. The slopes (1.11 to 1.32) are close to unity and much smaller than the slope expected from pure kinetics (2.81). A slope near unity is expected only if the evolution of the NMHC ratios is dominated by the mixing of fresh emissions into a ubiquitous background that contains significant concentrations of only the NMHC in the denominator, in this case benzene. The FLEXPART calculations in Figure 10 predict much more nearly kinetic behavior with slopes near 2.3. If mixing with a ubiquitous background is approximated by adding 100 pptv benzene to the FLEXPART calculated benzene levels for the WP-3D 2004 data set, then a slope of 1.43 is predicted, which is in reasonable agreement with the experimental pattern. However, this background is inconsistent with the measured benzene concentrations, which are frequently well below 100 pptv, as indicated by the color coding in Figure 9. It is unlikely that experimental problems can explain the behavior, since that behavior is common to the three different data sets. Further, the aromatic NMHC data from the WP-3D 2004 data set have been found [*de Gouw et al.*, 2006] to agree well with simultaneous measurements by an onboard proton-transfer reaction mass spectrometer system that made measurements in real time. No satisfactory explanation for the contrast between Figures 9 and 10 has been developed. What is clear, however, is that the behavior exhibited in Figure 9 is not consistent with photochemical processing by OH radicals (according to the rate constants of Table 1) of fresh emissions (characterized by the emission ratios of Table 1) and mixing as derived from the FLEXPART calculations.

[52] Figures 11 and 12 present the experimental and FLEXPART based model results for two aromatic ratios with toluene in the denominator. Figures 11 and 12 do not provide such a striking contrast. The experimental measurements give slopes significantly steeper than unity (1.8 to 2.5), but not as steep as the slopes predicted from the FLEXPART calculations (about 3.2). However, there is significant scatter in the relationships in the measurements that seems to be characteristic of the particular data set, although the r^2 values of the measured correlations (0.57 to 0.64) are not markedly worse than those modeled (0.84 to 0.87).

[53] The behavior of the aromatic ratios discussed with respect to Figures 9–12 is similar to the analysis of

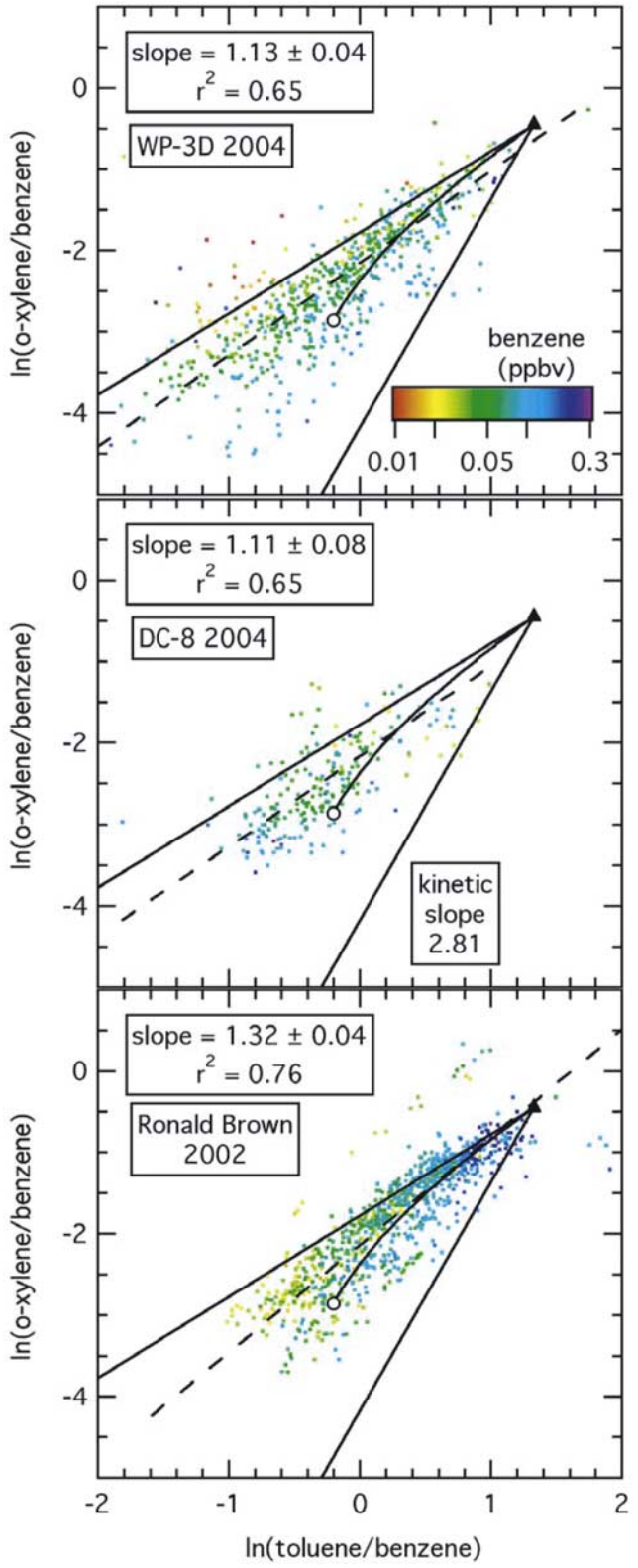

Figure 9. Correlation of the natural logarithms of two aromatic concentration ratios for samples collected during three aircraft field studies (dots), color coded according to the log of the benzene concentration. The format is the same as in Figure 2. The solid lines and symbols give limiting behavior discussed in the text.

de Gouw et al. [2005], which is based upon the *Ronald H. Brown* 2002 data set also considered here. Their Figure 3 shows that the ratios of various aromatics to benzene evolve at approximately the same rates, corresponding to the slope near unity in Figure 9 here. Further, their Figure 3 also shows that the ratios of the more reactive aromatics to toluene evolve more nearly as expected from the kinetic rate constants, corresponding to the slope greater than unity in Figure 11 here. *de Gouw et al.* [2005] suggest that the failure of the aromatic ratios to give accurate photochemical ages may be due to the mixing between more and less aged air masses. However, the treatment of mixing presented here indicates that additional, unknown factors are also influencing these ratios.

[54] The comparison between the measurements and the model is limited for the aromatics because of the experimental difficulties of determining the concentrations of the more reactive aromatics in aged air masses. For example in the DC-8 aircraft data set over 90% of the samples had one or more of the aromatics below the 3 pptv detection limit.

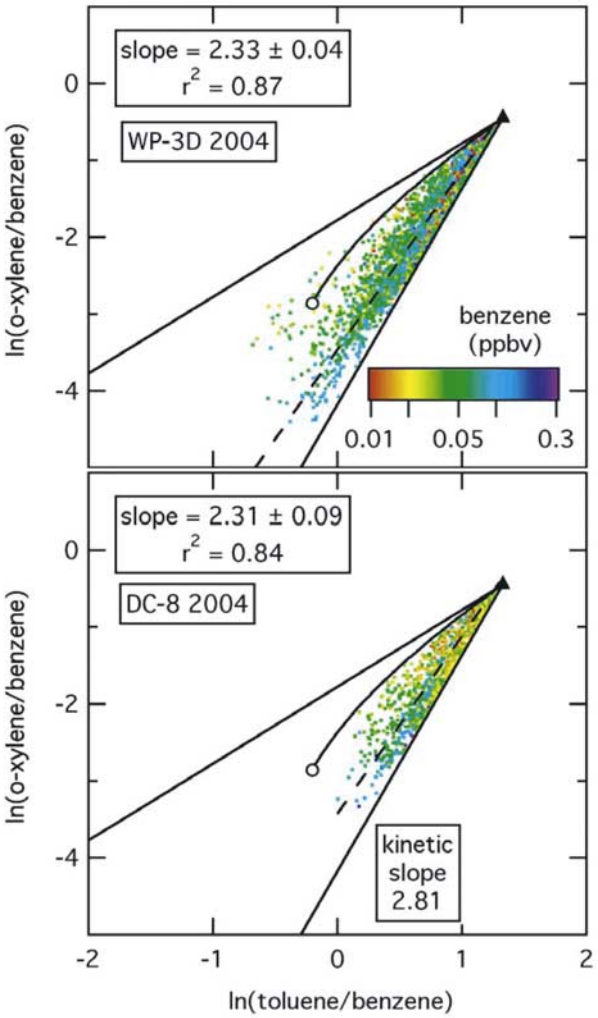

Figure 10. Correlation of the natural logarithms of two aromatic concentration ratios calculated from FLEXPART age spectra for two aircraft field studies (dots) in the same format as Figure 9.

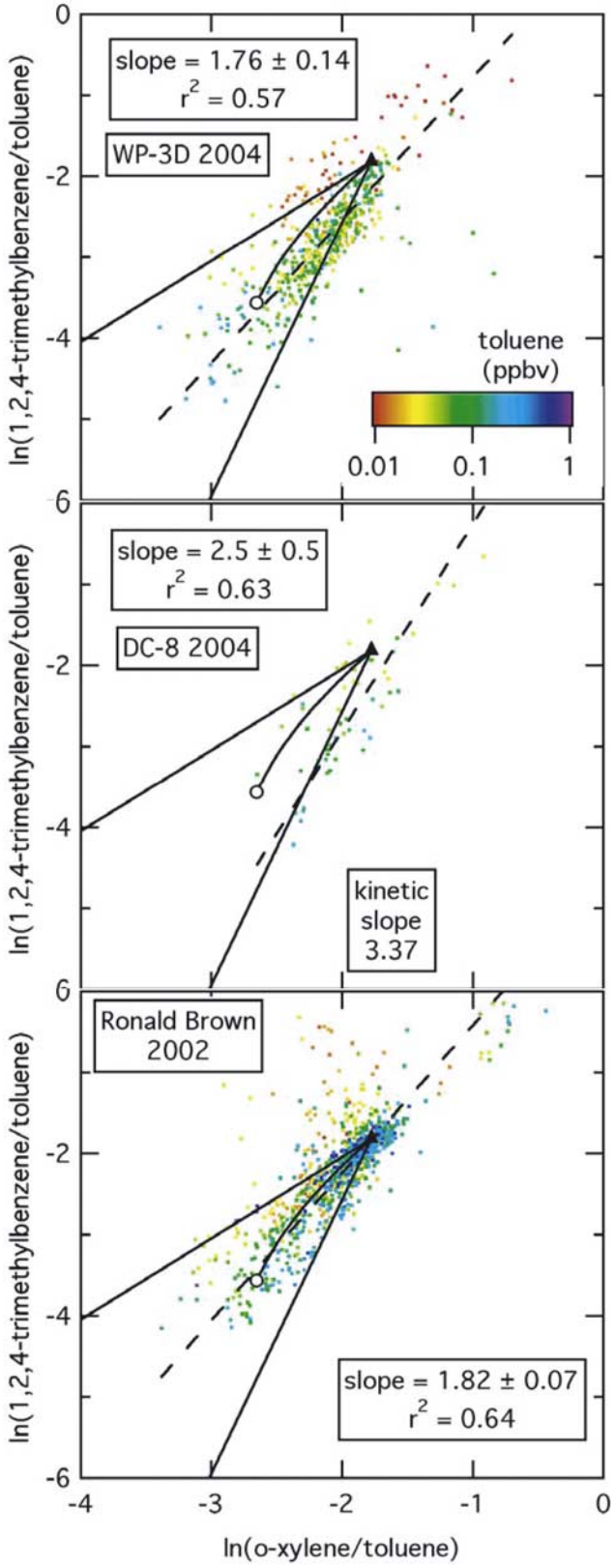

Figure 11. Correlation of the natural logarithms of two aromatic concentration ratios for samples collected during three field studies (dots), color coded according to the log of the toluene concentration. The format is the same as in Figure 2. The solid lines and symbols give limiting behavior discussed in the text.

The percent of data below the detection limit is well predicted by the FLEXPART calculations for both aircraft data sets (Table 3).

[55] In summary, the aromatic ratio comparisons between the measurements and the model suggest that the ratios provide robust qualitative indicators of photochemical processing. However, given the lack of understanding of some differences between the measurements and the model and the difficulty of measuring aromatics at low concentrations, care should be taken in the quantitative interpretation of aromatic NMHC ratios as indicators of photochemical processing.

5. Discussion and Conclusions

[56] The relationships between measured NMHC ratios in the troposphere have proven difficult to fully understand.

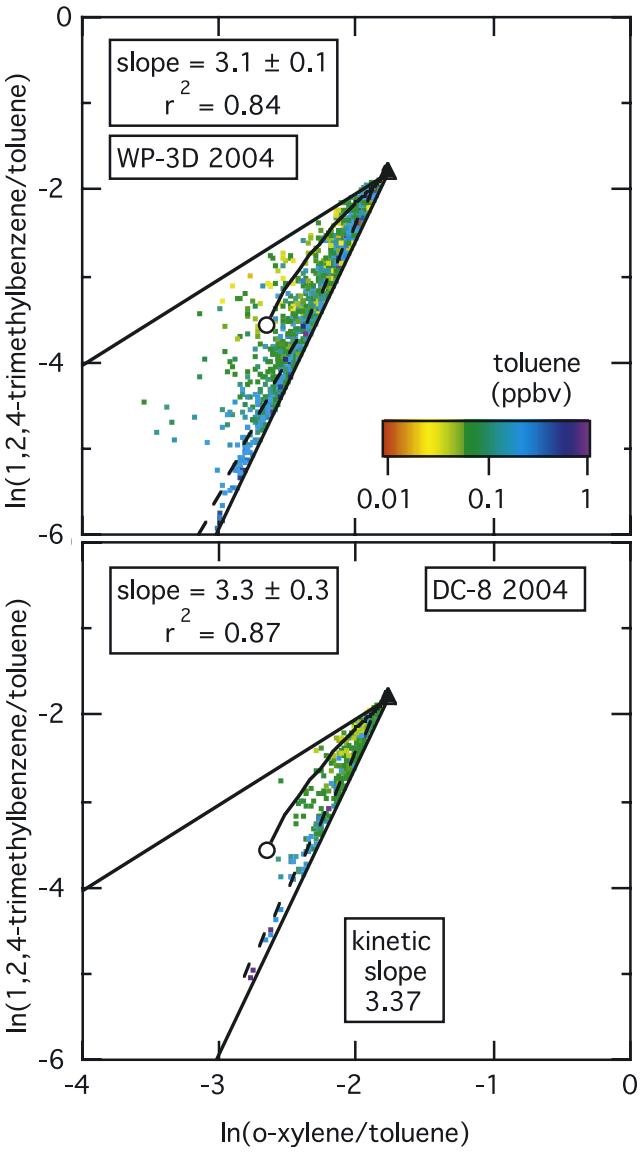

Figure 12. Correlation of the natural logarithms of two aromatic concentration ratios calculated from FLEXPART age spectra for two aircraft field studies (dots) in the same format as Figure 11.

They deviate from the behavior expected from pseudo-first-order attack by OH on each NMHC in an isolated air parcel. These deviations have been attributed to the effects of mixing of NMHC emitted at different times into any sampled air parcel. In the work reported here we develop a model for investigating the simultaneous effects of photochemical processing and mixing by combining a sophisticated transport treatment with an ultrasimple chemical treatment. The model gives NMHC relationships that can be directly compared, at least in a statistical manner, with the measured relationships.

[57] The Lagrangian particle dispersion model FLEXPART [*Stohl et al.*, 2005] is a state of the art model for representing atmospheric mixing and transport. To approximately treat the photochemical processing, a uniform, constant OH concentration is assumed throughout the troposphere, and rate constants for OH attack on the measured NMHC are taken from the literature. FLEXPART follows anthropogenic CO emissions, treated as an inert tracer, as they are transported and mixed within the atmosphere. We have used these results to represent NMHC by assuming each NMHC is emitted proportional to CO with proportionality constants taken from other studies.

[58] Since the treatment of the photochemistry in our model is very simplified (assumed uniform constant OH concentration), it is not possible to make a one-to-one comparison of the ratios measured in a particular NMHC sample to those calculated from the corresponding age spectrum. Rather we present statistical comparisons of the relationships between NMHC concentration ratios determined from measurements and derived from the model. The validity of these comparisons rests on the implicit assumption that the FLEXPART age spectra convoluted with a constant OH concentration provide an adequate representation of the true age spectra of the sampled air parcels convoluted with the true time-dependent OH concentrations to which the NMHC mixtures in the sampled air parcels have been exposed. This assumption is at least plausible. The FLEXPART calculations indicate that emissions from a wide range of sources emitted over a wide range of time are mixed into each sampled air parcel. These spatial and temporal ranges will tend to average out specific features associated with local phenomena, especially since we deal primarily with NMHC ratios rather than absolute concentrations. However, until a coupled chemical-Lagrangian particle dispersion model is developed, it will not be possible to rigorously test this assumption.

[59] Overall, the model calculations give good representations of the alkane ratio relationships, but a poorer representation of the aromatic ratio relationships. The measured concentrations of the longest-lived alkanes (Figure 2) give ratios that show strong deviations from purely kinetic behavior, and the model (Figure 5) nicely reproduces the observed behavior. The measurements and the model agree that the ratios formed from the C_3-C_5 alkanes (Figures 7 and 8) more closely follow purely kinetic behavior. In contrast, the measured aromatic ratio relationships with benzene in the denominator (Figure 9) are not well reproduced by the model (Figure 10) and the reasons for this are not understood. It is clear that the behavior exhibited in Figure 9 is not consistent with photochemical processing by OH radicals (according to the rate constants of Table 1) of freshly emitted aromatics (characterized by the emission ratios of Table 1) and dispersion and mixing as derived from the FLEXPART calculations. Reactions with chlorine atoms or NO_3 radicals also cannot explain this behavior. Better measurement-model agreement is seen for the aromatic ratios with toluene in the denominator, but the detection limits of the measurements become a more important limiting factor for these species.

[60] It is clear that the photochemical age as defined in equation (3) cannot be directly used as a quantitative measure for photochemical processing in a sampled air parcel. Nevertheless, NMHC ratios do give good qualitative to semiquantitative measures for the degree of that photochemical processing. They certainly do ''tick forward'' as photochemical processing proceeds. However, we point out that the photochemical age of an air parcel cannot be well defined if that parcel contains species of differing reactivity emitted at different times. A quantity that is well defined is the average age, given by equation (8), of any particular NMHC in a measured air parcel. Generally the average ages of NMHC in an air parcel can differ widely as indicated in Figure 6, and none is necessarily equal to the photochemical age calculated from an NMHC ratio through equation (3). However, it is generally possible to select an NMHC ratio that yields a photochemical age in reasonable accord (at least within 50%) with the average age of a given NMHC.

[61] The treatment presented here differs in one important respect from earlier efforts to give a semiquantitative treatment of the interaction of mixing and aging. *McKeen and Liu* [1993] and *McKeen et al.* [1996] approximately reproduced the alkane ratio relationship of Figure 2 by mesoscale model calculations that simultaneously treated the photochemical processing of the NMHC and their dilution by background air. This approach required the definition of ''background'' concentrations of the NMHC of interest. In effect, they used a ''two-point'' approach: one assumed point is the ''background'' concentration ratios, and the other is the emission ratios of the NMHC. The model then reproduced the NMHC ratio relationships between these two points. In contrast, the treatment presented in this work is a ''one-point'' approach: only the emission ratios are assumed. The model reproduces the evolution of the NMHC ratio relationship from that one point to the most aged air parcels encountered; the concept of ''background'' concentrations never arises. Indeed, ''background'' concentration is a poorly defined concept. In the approach taken here, there is no lower limit to a NMHC concentration. Even in the ''two-point'' approach the ''background'' definition was problematic, as an air parcel initially at the defined NMHC background concentrations, evolved to lower concentrations during the model calculation when it was sufficiently isolated from the addition of fresher emissions.

[62] Utilization of NMHC ratios to yield a measure of photochemical processing is a useful analytic tool; however, the relationships of NMHC ratios may well be more useful as tests of the treatment of the interaction of mixing and chemical processing in chemical transport models. Reproduction of the relationships investigated in this paper are likely to provide severe tests of more sophisticated models than that used in this work. A start in this direction has been made by *Wang and Zeng* [2004] who used the observed and modeled relationship between propane and the ethane/

propane ratio as a diagnostic of the treatment of transport in their GEOS-CHEM model.

[63] **Acknowledgments.** The Climate Change and Air Quality Programs of NOAA supported the WP-3D and Research Vessel *Ronald H. Brown* measurements and the analysis. The NASA Tropospheric Chemistry Program supported the DC-8 activities.

References

Atkinson, R., and J. Arey (2003), Atmospheric degradation of volatile organic compounds, *Chem. Rev.*, *103*, 4605–4638.

Blake, D. R., et al. (1996), Nonmethane hydrocarbon and halocarbon distributions during Atlantic Stratocumulus Transition Experiment/Marine Aerosol and Gas Exchange, June 1992, *J. Geophys. Res.*, *101*, 4501–4514.

Blake, N. J., et al. (2003), NMHCs and halocarbons in Asian continental outflow during the Transport and Chemical Evolution over the Pacific (TRACE-P) Field Campaign: Comparison With PEM-West B, *J. Geophys. Res.*, *108*(D20), 8806, doi:10.1029/2002JD003367.

Broecker, W. S., and T.-H. Peng (1982), *Tracers in the Sea*, Lamont-Doherty Geol. Obs., Columbia Univ., Palisades, N. Y.

Brost, R. A., and M. Heimann (1991), The effect of global background on a synoptic-scale simulation of tracer concentration, *J. Geophys. Res.*, *96*(D8), 15,415–15,425.

Calvert, J. G. (1976), Hydrocarbon involvement in photochemical smog formation in Los Angeles atmosphere, *Environ. Sci. Technol.*, *10*, 256–262.

de Gouw, J. A., et al. (2005), Budget of organic carbon in a polluted atmosphere: Results from the New England Air Quality Study in 2002, *J. Geophys. Res.*, *110*, D16305, doi:10.1029/2004JD005623.

de Gouw, J. A., et al. (2006), Volatile organic compounds composition of merged and aged forest fire plumes from Alaska and western Canada, *J. Geophys. Res.*, *111*, D10303, doi:10.1029/2005JD006175.

Ehhalt, D. H., F. Rohrer, A. Wahner, M. J. Prather, and D. R. Blake (1998), On the use of hydrocarbons for the determination of tropospheric OH concentrations, *J. Geophys. Res.*, *103*(D15), 18,981–18,998.

Fehsenfeld, F. C., et al. (2006), International Consortium for Atmospheric Research on Transport and Transformation (ICARTT): North America to Europe—Overview of the 2004 summer field study, *J. Geophys. Res.*, *111*, D23S01, doi:10.1029/2006JD007829.

Forster, C., et al. (2004), Lagrangian transport model forecasts and a transport climatology for the Intercontinental Transport and Chemical Transformation 2002 (ITCT 2k2) measurement campaign, *J. Geophys. Res.*, *109*, D07S92, doi:10.1029/2003JD003589.

Frost, G. J., et al. (2006), Effects of changing power plant NO_x emissions on ozone in the eastern United States: Proof of concept, *J. Geophys. Res.*, *111*, D12306, doi:10.1029/2005JD006354.

Goldan, P. D., W. C. Kuster, E. Williams, P. C. Murphy, F. C. Fehsenfeld, and J. Meagher (2004), Nonmethane hydrocarbon and oxy hydrocarbon measurements during the 2002 New England Air Quality Study, *J. Geophys. Res.*, *109*, D21309, doi:10.1029/2003JD004455.

Goldstein, A. H., et al. (1995), Seasonal variations of nonmethane hydrocarbons in rural New England: Constraints on OH concentrations in northern midlatitudes, *J. Geophys. Res.*, *100*, 21,023–21,033.

Hoell, J. M., et al. (1997), The Pacific Exploratory Mission–West Phase B: February–March, 1994, *J. Geophys. Res.*, *102*, 28,223–28,239.

Jobson, B. T., et al. (1994a), Measurements of C_2–C_6 hydrocarbons during the Polar Sunrise 1992 Experiment: Evidence for Cl atom and Br atom chemistry, *J. Geophys. Res.*, *99*, 25,355–25,368.

Jobson, B. T., et al. (1994b), Seasonal trends of isoprene, C_2–C_5 alkanes, and acetylene at a remote boreal site in Canada, *J. Geophys. Res.*, *99*, 1589–1599.

Kleinman, L. I., et al. (2003), Photochemical age determinations in the Phoenix metropolitan area, *J. Geophys. Res.*, *108*(D3), 4096, doi:10.1029/2002JD002621.

McKeen, S. A., and S. C. Liu (1993), Hydrocarbon ratios and photochemical history of air masses, *Geophys. Res. Lett.*, *20*, 2363–2366.

McKeen, S. A., et al. (1990), On the indirect determination of atmospheric OH radical concentrations from reactive hydrocarbon measurements, *J. Geophys. Res.*, *95*, 7493–7500.

McKeen, S. A., et al. (1996), Hydrocarbon ratios during PEM-West A: A model perspective, *J. Geophys. Res.*, *101*, 2087–2109.

McKenna, D. S. (1997), Analytic solutions of reaction diffusion equations and implications for the concept of an air parcel, *J. Geophys. Res.*, *102*, 13,719–13,726.

McKenna, D. S., C. J. Hord, and J. M. Kent (1995), Hydroxyl radical concentrations and Kuwait oil fire emission rates for March 1991, *J. Geophys. Res.*, *100*(D12), 26,005–26,026.

Neri, F., G. Saitta, and S. Chiofalo (1989), An accurate and straightforward approach to line regression analysis of error-affected experimental data, *J. Phys. E Sci. Instrum*, *22*, 215–217.

Parrish, D. D., et al. (1992), Indications of photochemical histories of Pacific air masses from measurements of atmospheric trace species at Pt. Arena, California, *J. Geophys. Res.*, *97*, 15,883–15,901.

Parrish, D. D., et al. (1998), Internal consistency tests for evaluation of measurements of anthropogenic hydrocarbons in the troposphere, *J. Geophys. Res.*, *103*, 22,339–22,359.

Parrish, D. D., Y. Kondo, O. R. Cooper, C. A. Brock, D. A. Jaffe, M. Trainer, T. Ogawa, G. Hübler, and F. C. Fehsenfeld (2004a), Intercontinental Transport and Chemical Transformation 2002 (ITCT 2K2) and Pacific Exploration of Asian Continental Emission (PEACE) experiments: An overview of the 2002 winter and spring intensives, *J. Geophys. Res.*, *109*, D23S01, doi:10.1029/2004JD004980.

Parrish, D. D., et al. (2004b), Changes in the photochemical environment of the temperate North Pacific troposphere in response to increased Asian emissions, *J. Geophys. Res.*, *109*, D23S18, doi:10.1029/2004JD004978.

Press, W. H., S. A. Teukolsky, W. T. Vetterling, and B. P. Flannery (1992), *Numerical Recipes in C*, 2nd ed., Cambridge Univ. Press, New York.

Roberts, J. M., et al. (1984), Measurements of aromatic hydrocarbon ratios and NOX concentration in the rural troposphere: Observation of air mass photochemical aging and NOX removal, *Atmos. Environ.*, *18*, 2421–2432.

Roberts, J. M., et al. (1985), Measurements of anthropogenic hydrocarbon concentration ratios in the rural troposphere: Discrimination between background and urban sources, *Atmos. Environ.*, *19*, 1945–1950.

Rudolph, J., and F. J. Johnen (1990), Measurements of light atmospheric hydrocarbons over the Atlantic in regions of low biological activity, *J. Geophys. Res.*, *95*, 20,583–20,591.

Schauffler, S. M., E. L. Atlas, D. R. Blake, F. Flocke, R. A. Lueb, J. M. Lee-Taylor, V. Stroud, and W. Travnicek (1999), Distributions of brominated organic compounds in the troposphere and lower stratosphere, *J. Geophys. Res.*, *104*(D17), 21,513–21,535.

Schauffler, S. M., E. L. Atlas, S. G. Donnelly, A. Andrews, S. A. Montzka, J. W. Elkins, D. F. Hurst, P. A. Romashkin, G. S. Dutton, and V. Stroud (2003), Chlorine budget and partitioning during the Stratospheric Aerosol and Gas Experiment (SAGE) III Ozone Loss and Validation Experiment (SOLVE), *J. Geophys. Res.*, *108*(D5), 4173, doi:10.1029/2001JD002040.

Spivakovsky, C. M., et al. (2000), Three dimensional climatological distribution of tropospheric OH: Update and evaluation, *J. Geophys. Res.*, *105*, 8931–8980.

Stohl, A., S. Eckhardt, C. Forster, P. James, and N. Spichtinger (2002), On the pathways and timescales of intercontinental air pollution transport, *J. Geophys. Res.*, *107*(D23), 4684, doi:10.1029/2001JD001396.

Stohl, A., C. Forster, S. Eckhardt, N. Spichtinger, H. Huntrieser, J. Heland, H. Schlager, S. Wilhelm, F. Arnold, and O. Cooper (2003), A backward modeling study of intercontinental pollution transport using aircraft measurements, *J. Geophys. Res.*, *108*(D12), 4370, doi:10.1029/2002JD002862.

Stohl, A., C. Forster, A. Frank, P. Seibert, and G. Wotawa (2005), Technical note: The Lagrangian particle dispersion model FLEXPART version 6.2, *Atmos. Chem. Phys.*, *5*, 2461–2474.

Swanson, A. L., N. J. Blake, E. Atlas, F. Flocke, D. R. Blake, and F. S. Rowland (2003), Seasonal variations of C_2–C_4 nonmethane hydrocarbons and C_1–C_4 alkyl nitrates at the Summit research station in Greenland, *J. Geophys. Res.*, *108*(D2), 4065, doi:10.1029/2001JD001445.

Wang, Y., and T. Zeng (2004), On tracer correlations in the troposphere: The case of ethane and propane, *J. Geophys. Res.*, *109*, D24306, doi:10.1029/2004JD005023.

Warneke, C., et al. (2004), Comparison of daytime and nighttime oxidation of biogenic and anthropogenic VOCs along the New England coast in summer during New England Air Quality Study 2002, *J. Geophys. Res.*, *109*, D10309, doi:10.1029/2003JD004424.

E. L. Atlas, Division of Marine and Atmospheric Chemistry, Rosenstiel School of Marine and Atmospheric Science, University of Miami, Miami, FL 33149, USA.

D. R. Blake, Department of Chemistry, University of California, Irvine, CA 92697-2025, USA.

J. A. de Gouw, P. D. Goldan, W. C. Kuster, and D. D. Parrish, Earth System Research Laboratory, NOAA, 325 Broadway R/CSD7, Boulder, CO 80305, USA. (david.d.parrish@noaa.gov)

C. Forster and A. Stohl, Department of Regional and Global Pollution Issues, Norwegian Institute for Air Research, P.O. Box 100, N-2027 Kjeller, Norway.